

The LTP Experiment on the LISA Pathfinder Mission

Anza S¹, Armano M², Balaguer E³, Benedetti M⁴, Boatella C¹, Bosetti P⁴, Bortoluzzi D⁴, Brandt N⁵, Braxmaier C⁵, Caldwell M⁶, Carbone L², Cavalleri A², Ciccolella A³, Cristofolini I⁴, Cruise M⁷, Da Lio M⁴, Danzmann K⁸, Desiderio D⁹, Dolesi R², Dunbar N¹⁰, Fichter W⁵, Garcia C³, Garcia-Berro E¹¹, Garcia Marin A F⁸, Gerndt R⁵, Gianolio A³, Giardini D¹², Gruenagel R³, Hammesfahr A⁵, Heinzl G⁵, Hough J¹³, Hoyland D⁷, Hueller M², Jennrich O³, Johann U⁵, Kemble S¹⁰, Killow C¹³, Kolbe D⁵, Landgraf M¹⁴, Lobo A¹⁵, Lorizzo V⁹, Mance D¹², Middleton K⁶, Nappo F⁹, Nofrarias M¹, Racca G³, Ramos J¹¹, Robertson D¹³, Sallusti M³, Sandford M⁶, Sanjuan J¹, Sarra P⁹, Selig A¹⁶, Shaul D¹⁷, Smart D⁶, Smit M¹⁶, Stagnaro L³, Sumner T¹⁷, Tirabassi C³, Tobin S⁶, Vitale S^{2,†}, Wand V⁸, Ward H¹³, Weber W J², Zweifel P¹²

¹ Institut d'Estuds Espacials de Catalunya, Barcelona, Spain

² Department of Physics and INFN, University of Trento, 38050 Povo (TN), Italy

³ ESA-ESTEC, 2200 AG Noordwijk (The Netherlands)

⁴ Department of Mechanical and Structural Engineering, University of Trento, 38050 Trento, Italy

⁵ EADS Astrium GmbH, Friedrichshafen, Immenstaad 88090, Germany

⁶ Rutherford Appleton Laboratory, Chilton-Didcot, UK

⁷ Department of Physics & Astronomy, University of Birmingham, UK

⁸ Max-Planck-Institut für Gravitationsphysik (Albert-Einstein-Institut) and Universität Hannover, Hannover, Germany

⁹ Carlo Gavazzi Space, 20151 Milano, Italy

¹⁰ EADS Astrium Ltd, Stevenage, Hertfordshire, SG1 2AS, UK

¹¹ Univeritat Politecnica de Catalunya, Barcelona, Spain

¹² Swiss Federal Institute of Technology Zurich, Geophysics, CH-8093 Zürich

¹³ Department of Physics and Astronomy, University of Glasgow, Glasgow, UK

¹⁴ ESA/ESOC, 64293 Darmstadt, Germany

¹⁵ Universidad de Barcelona, Barcelona 08028 Spain

¹⁶ SRON National Institute for Space Research, 3584 CA Utrecht, the Netherlands

¹⁷ The Blackett Laboratory, Imperial College of Science, Technology & Medicine, London, UK

Abstract. We report on the development of the LISA Technology Package (LTP) experiment that will fly on board the LISA Pathfinder mission of the European Space Agency in 2008. We first summarize the science rationale of the experiment aimed at showing the operational feasibility of the so called Transverse-Traceless coordinate frame within the accuracy needed for LISA. We then show briefly the basic features of the instrument and we finally discuss its projected sensitivity and the extrapolation of its results to LISA.

† Corresponding author: Stefano.Vitale@unitn.it

1. Introduction

Our very concept of the detection of gravitational wave by an interferometric detector like LISA [1, 2] is based on the operative possibility of realizing a Transverse and Traceless (TT) coordinate frame [3].

In this kind of coordinate frame, despite the presence of the ripple in space-time curvature due to the gravitational wave, a free particle initially at rest remains at rest, i.e. its space coordinates do not change in time, and the proper time of a clock sitting on the particle coincides with the coordinate time.

Despite the co-moving nature of such a frame, the distances among particles at rest change in time because of the change of the metric tensor, and this time variation can be detected by the laser interferometer.

Indeed a laser beam travelling back and forth between two such particles along an axis \mathbf{x} normal to the direction \mathbf{z} of the gravitational wave propagation, is subject to a phase shift $\delta\theta(t)$ whose time derivative is given $\delta\nu/\nu_o$ by [3]:

$$\frac{d\delta\theta}{dt} = \frac{\pi c}{\lambda} \left[h_+ \left(t - \frac{2L}{c} \right) - h_+(t) \right]. \quad (1)$$

Here h_+ is the usual definition [3] for the amplitude of the wave, L is the distance between the particles and λ is the wavelength of the laser. Furthermore the \mathbf{x} -axis has been used to define the wave polarization, so that the phase shift is only contributed by h_+ , and t is the time at which light is collected and the frequency shift is measured.

As all this holds within a linearized theory, small effects superimpose and harmonic analysis can be applied. As a consequence secular gravitational effects at frequencies much lower than the observation bandwidth ($f < 10^{-4}$ Hz) do not matter. A TT coordinate frame may then in principle be defined just for the frequencies of relevance, letting the particles used to mark the frame to change their coordinates at lower frequencies because of their motion within the gravitational field of the Solar System.

If the particles are not at rest in the TT frame, i.e. if their space coordinates change in time, then obviously their distances will change also because of this motion. If the particles still move slowly relative to light, their relative motion does not affect the TT construction but competes with the signal in (1) by providing a phase shift:

$$\delta\theta(t) = \frac{2\pi}{\lambda} \left\{ x_1(t) + x_1 \left(t - \frac{2L}{c} \right) - 2x_2 \left(t - \frac{L}{c} \right) \right\} \quad (2)$$

where x_1 is the coordinate of the particle sending and collecting the laser beam, while x_2 is that of the particle reflecting the light. Here coordinates are components along the laser beam and the phase shift is calculated to first order in v/c .

At measurement frequencies much lower than c/L (2) gives obviously

$$\delta\theta(t) \approx \frac{4\pi}{\lambda} \Delta L(t) \quad \text{with} \quad \Delta L(t) = x_1(t) - x_2(t). \quad (3)$$

If all coordinates may be assumed as joint stationary random processes, the phase shift in (3) has a Power Spectral Density (PSD)

$$\begin{aligned} S_{\delta\theta}(\omega) &= \frac{16\pi^2}{\lambda^2} \left\{ S_{\Delta L}(\omega) \left[1 - 2 \sin^2 \left(\frac{\omega L}{2c} \right) \right] + \right. \\ &\quad \left. + 8 \sin^2 \left(\frac{\omega L}{2c} \right) \left[S_{x_2}(\omega) - \cos \left(\frac{\omega L}{c} \right) S_{x_1}(\omega) \right] \right\} \\ &\approx \frac{16\pi^2}{\lambda^2} S_{\Delta L}(\omega) \end{aligned} \quad (4)$$

where $S_{\Delta L}(\omega)$, $S_{x_2}(\omega)$, and $S_{x_1}(\omega)$ are the PSD of the related quantities at angular frequency ω and the rightmost approximate equality holds for $|\omega| L/c \ll 1$.

In a TT frame, and at low velocities, the motion of proof-masses can only be caused by forces that are not due to the gravitational wave. Equation (4) then becomes:

$$S_{\delta\theta} \approx \frac{16\pi^2}{\lambda^2} \frac{S_{\Delta F}}{\omega^4 m^2} \quad (5)$$

where $S_{\Delta F}$ is the spectral density of the *difference* of force between the proof-masses.

Thus to show that a TT system can indeed be constructed with free orbiting particles, one needs to preliminarily show that non-gravitational forces on proof-masses, or even locally generated gravitational forces, can be suppressed to the required accuracy in the measurement bandwidth.

The interferometer measurement noise will also compete with the gravitational signal in (1). This noise is usually expressed as an equivalent optical path fluctuation δx for each passage of the light through the interferometer arm. For such an optical path fluctuation, our single-arm interferometer would suffer a phase shift

$$\delta\theta(t) \approx \frac{2\pi}{\lambda} \delta x(t) \quad (6)$$

each way. As a consequence, if the PSD of δx is S_x , this noise source would add an equivalent phase noise

$$S_{\delta\theta} \approx 2 \frac{4\pi^2}{\lambda^2} S_x. \quad (7)$$

In LISA the targeted sensitivity [1] requires that $S_{\Delta F}^{1/2}(\omega)/m^2 \leq \sqrt{2} \cdot 3 \times 10^{-15} (\text{m/s}^2)/\sqrt{\text{Hz}}$ for a frequency f above $f > 0.1$ mHz. The corresponding requirement for the interferometer is a path-length noise spectrum of $S_x^{1/2} \leq 20 \text{ pm}/\sqrt{\text{Hz}}$. With these figure the noise in (5) and that in (7) cross at ≈ 3 mHz thus allowing to relax the requirement for $\Delta F/m$ to:

$$\begin{aligned} S_{\Delta F/m}^{1/2} &\leq \sqrt{2} \times 3 \times 10^{-15} \frac{\text{m}}{\text{s}^2 \sqrt{\text{Hz}}} \sqrt{1 + \left(\frac{f}{3\text{mHz}}\right)^4} \\ &\approx 4.2 \times 10^{-15} \frac{\text{m}}{\text{s}^2 \sqrt{\text{Hz}}} \left[1 + \left(\frac{f}{3\text{mHz}}\right)^2 \right] \end{aligned} \quad (8)$$

The requirement in (8) needs to be qualified. Limiting the noise in (4) by a requirement just for the differential force noise becomes inaccurate at frequencies above some 3-4 mHz. However, if the velocity fluctuations of the two proof-masses are independent, this approach represents a *worst case* one. This is also the case for a partly correlated noise, provided that correlation is assumed to work in the worst direction, i.e. by mimicking differential motion.

The focus of the above discussion has been in term of coordinate frames. One can however restate these performance requirements in terms of coordinate independent, or gauge invariant quantities, i.e. in term of the curvature tensor $R_{\mu\nu\sigma}^\lambda$ only.

For a gravitational wave, the curvature tensor is equal, in the Fourier domain, to

$$R_{\mu\nu\sigma}^{\lambda} = \frac{\omega^2}{2c^2} \begin{pmatrix} \vec{0} & \vec{H}_+ & \vec{H}_\times & \vec{0} \\ \vec{H}_+ & \vec{0} & \vec{0} & -\vec{H}_+ \\ \vec{H}_\times & \vec{0} & \vec{0} & -\vec{H}_\times \\ \vec{0} & \vec{H}_+ & \vec{H}_\times & \vec{0} \end{pmatrix} \quad (9)$$

with

$$\vec{H}_+ = \begin{pmatrix} 0 & -h_+(\omega) & -h_\times(\omega) & 0 \\ h_+(\omega) & 0 & 0 & -h_+(\omega) \\ h_\times(\omega) & 0 & 0 & -h_\times(\omega) \\ 0 & h_+(\omega) & h_\times(\omega) & 0 \end{pmatrix}$$

and

$$\vec{H}_\times = \begin{pmatrix} 0 & -h_\times(\omega) & h_+(\omega) & 0 \\ h_\times(\omega) & 0 & 0 & -h_\times(\omega) \\ -h_+(\omega) & 0 & 0 & h_+(\omega) \\ 0 & h_\times(\omega) & -h_+(\omega) & 0 \end{pmatrix} \quad (10)$$

For $|\omega| L/2 \ll 1$ and for an optimally oriented ($\phi=0$) interferometer arm the phase shift in (1) can then be written as:

$$\delta\theta(\omega) \approx \frac{2\pi}{\lambda} L h_+(\omega) \approx \frac{2\pi}{\lambda} 2c^2 L \frac{R(\omega)}{\omega^2} \quad (11)$$

with R the generic component of the curvature tensor.

By comparing (11) with (8) $S_h^{1/2}(\omega) \approx \frac{2}{\omega^2 L} S_{\Delta F/m}^{1/2}$ one can recast the differential force noise as an effective curvature noise with spectrum:

$$S_R^{1/2}(\omega) \approx \frac{1}{c^2 L} S_{\Delta F/m}^{1/2} \quad (12)$$

Thus to achieve its science goals, LISA must reach a curvature resolution of order $10^{-41} \text{ m}^{-2}/\sqrt{\text{Hz}}$ or of 10^{-43} m^{-2} for a signal at 0.1 mHz integrated over a cycle. This figure may be compared with the scale of the curvature tensor due to the gravitational field of the Sun at the LISA location of $\approx 10^{-30} \text{ m}^{-2}$.

The aim of LISA Pathfinder mission of the European Space Agency (ESA) is to demonstrate that indeed a TT frame may be constructed by using particles nominally free orbiting within the solar system, with accuracy relevant for LISA. Specifically within the LISA Technology Package (LTP)[§], two LISA-like proof-masses located inside a single spacecraft are tracked by a laser interferometer. This minimal instrument is deemed to contain the essence of the construction procedure needed for LISA and thus to demonstrate its feasibility. This demonstration requires two steps:

- Firstly, based on a noise model [4, 5], the mission is designed so that any differential parasitic acceleration noise of the proof-masses is kept below the requirements. For the LTP these requirements are relaxed to $3 \times 10^{-14} \text{ ms}^{-2}/\sqrt{\text{Hz}}$, a factor ≈ 7 larger than what is required in LISA. In addition this performance is

[§] The LTP is a collaboration between ESA, and the space Agencies of Germany (DLR), Italy (ASI), The Netherlands (SRON), Spain (MEC), Switzerland (SSO) and United Kingdom (PPARC). In addition France (CNES/CNRS) is in the process of joining the team.

only required for frequencies larger than 1 mHz. This relaxation of performance is accepted in view of cost and time saving.

As both for LISA and for the LTP this level of performance cannot be verified on ground due to the presence of the large Earth gravity, the verification is mostly relying on the measurements of key parameters of the noise model of the instrument [6, 7, 8, 9, 10]. In addition an upper limit to all parasitic forces that act at the proof-mass surface (electrostatics and electromagnetics, thermal and pressure effects etc.) has been established and keeps being updated by means of a torsion pendulum test-bench [7, 11, 12]. In this instrument a hollow version of the proof-mass hangs from the torsion fiber of the pendulum so that it can freely move in a horizontal plane within a housing which is representative of flight conditions. An equivalent differential acceleration noise of $\approx 3 \times 10^{-13} \text{ms}^{-2}/\sqrt{\text{Hz}}$ has been measured [7].

- Secondly, once in orbit the residual differential acceleration noise of the proof-masses is measured. The noise model [13, 14] predicts that the contributions to the total PSD fall into three broad categories:
 - Noise sources whose effect can be identified and suppressed by a proper adjustment of selected instrument parameters. An example of this is the force due to residual coupling of proof-masses to the spacecraft. By regulating and eventually matching, throughout the application of electric field, the stiffness of this coupling for both proof-masses, this source of noise can be first highlighted, then measured, and eventually suppressed [14].
 - Noise sources connected to measurable fluctuations of some physical parameter. Forces due to magnetic fields or to thermal gradients are typical examples. The transfer function between these fluctuations and the corresponding differential proof-mass acceleration fluctuations will be measured by purposely enhancing the variation of the physical parameter under investigation [14] and by measuring the corresponding acceleration response. For instance the LTP carries magnetic coils to apply comparatively large magnetic field signals and heaters to induce time-varying thermal gradients. In addition the LTP also carries sensors to measure the fluctuation of the above physical disturbances while measuring the residual differential acceleration noise in the absence of any applied perturbation. Examples of these sensors are magnetometers and thermometers to continue with the examples above. By multiplying the measured transfer function by the measured disturbance fluctuations, one can generate an expected acceleration noise data stream to be subtracted from the main differential acceleration data stream. This way the contributions of these noise sources are suppressed and the residual acceleration PSD decreased. This reduction is obtained without requiring expensive magnetic “cleanliness”, or thermal stabilization programs.
 - Noise sources that cannot be removed by any of the above methods. The residual differential acceleration noise due to these sources must be accounted for [14]. To be able to do the required comparison, some of the noise model parameters must and will be measured in-flight. One example for all, the charged particle flux due to cosmic rays will be continuously monitored by a particle detector.

The result of the above procedure is the validation of the noise model for LISA and the

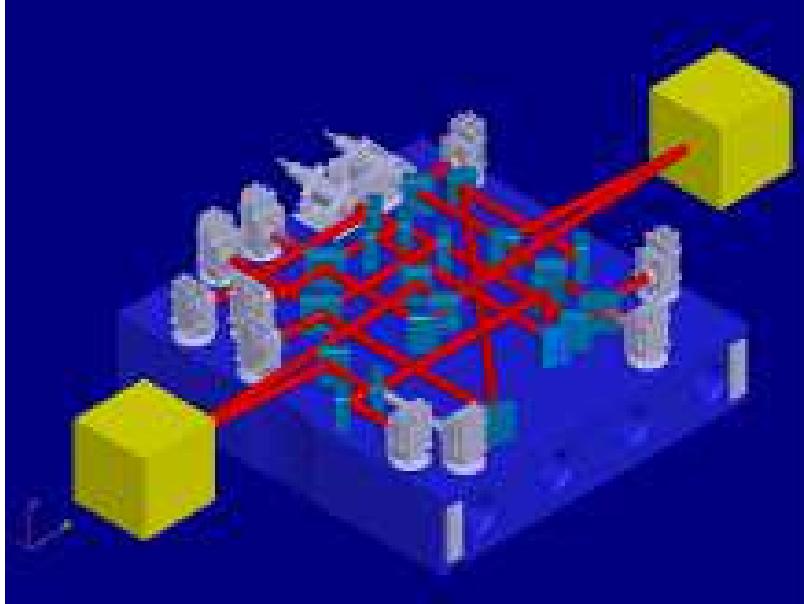


Figure 1. The concept of the LTP: The distance between 2 cubic, free floating proof-masses is measured by a heterodyne laser interferometer. The proof-masses centers nominal separation is $L=376$ mm, the proof-mass size is 46 mm and the mass value is 1.96 kg.

demonstration that no unforeseen source of disturbance is present that exceeds the residual uncertainty on the measured PSD. The following sections, after describing some details of the experiment, will discuss the expected amount of this residual uncertainty.

2. The LISA Technology Package experiment

The basic scheme of the LTP has been described in [2] and is shown in figure 1: two free-floating proof-masses are hosted within a single spacecraft and the relative motion along a common sensitive axis, the x -axis, is measured by means of a laser interferometer. The proof-masses are made of a Gold-Platinum, low magnetic susceptibility alloy, have a mass of $m = 1.96$ kg and are separated by a nominal distance of 376 mm. A picture of the instrument in its current stage of design and a few pictures of a prototype under development are reported from figure 2 to figure 4. In the following section we summarize the basic elements.

2.1. The LTP instrument

In the LTP, as in LISA, each proof-mass is surrounded by a set of electrodes that are used to readout the mass position and orientation relative to the spacecraft [11, 12, 15, 16] (figure 3). This measurement is obtained as the motion of the proof-mass varies the capacitances between the electrodes and the proof-mass itself. The same set of electrodes is also used to apply electrostatic forces to the proof-masses.

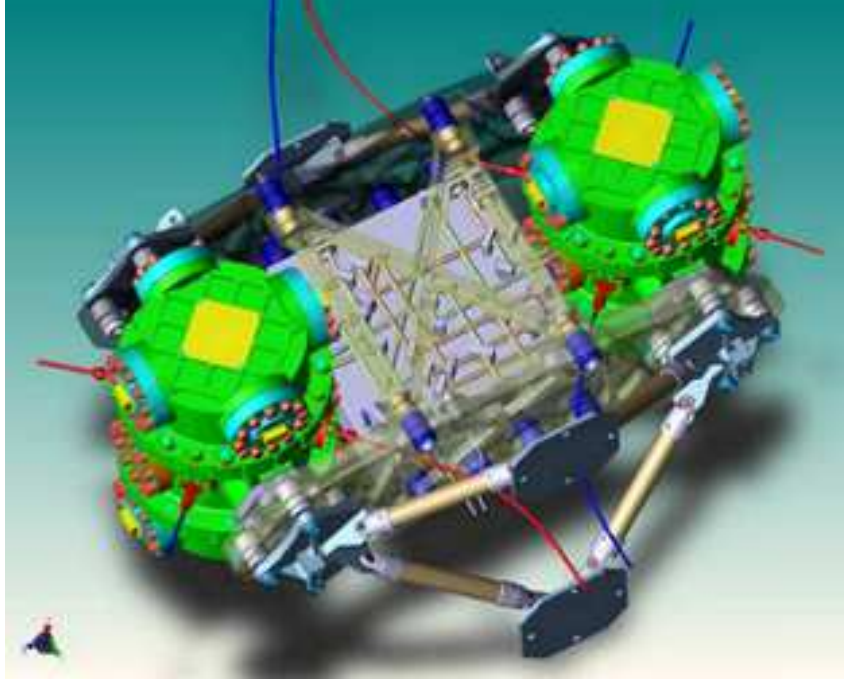


Figure 2. The LISA Technology Package. The green chambers are the vacuum enclosures that provide autonomous ultra-high vacuum around the proof-masses (non visible). An optical bench in between the proof-masses (in grey) supports the interferometry that reads out the distance between the masses. The interferometer laser beam hits each proof-mass by crossing the vacuum enclosures through an optical window. The entire supporting structure is made out of glass-ceramics for high thermo-mechanical stability. The red and blue lines are the optical fibers that carry the UV light used for contact-less discharging of proof-masses. Also visible are the side struts that connect the LTP to the spacecraft

Differential capacitance variations are parametrically read out by a front-end electronics composed of high accuracy differential inductive bridges excited at about 100 kHz, and synchronously detected via a phase sensitive detector [15, 17]. Sensitivities depend on the degree of freedom. For the x -axis it is better than $1.8 \text{ nm}/\sqrt{\text{Hz}}$ at 1 mHz. Angular sensitivities are better than $200 \text{ nrad}/\sqrt{\text{Hz}}$.

Forces and torques on the proof-masses required during science operation are applied through the same front-end electronics by modulating the amplitude of an ac carrier applied to the electrodes. The frequency of the carrier is high enough to prevent the application of unwanted forces by mixing with low frequency fluctuating random voltages. The front end electronics is also used to apply all voltages required by specific experiments [17].

Each proof-mass, with its own electrode housing, is enclosed in a high vacuum chamber which is pumped down to 10^{-5} Pa by a set of getter pumps. The laser interferometer light passes through vacuum chamber wall through an optical window.

As the proof-mass has no mechanical contact to its surrounding, its electrical charge continues to build up due to cosmic rays. To discharge the proof-mass, an ultra-violet light is shone on it and/or on the surrounding electrodes [18]. Depending



Figure 3. A prototype of the gravity reference sensor under development. Top left: the gold-platinum proof-mass. Bottom left: the electrode housing carrying the Gold-coated ceramics electrodes. Right: the vacuum enclosure. The optical windows for the laser light are substituted by plane flanges.

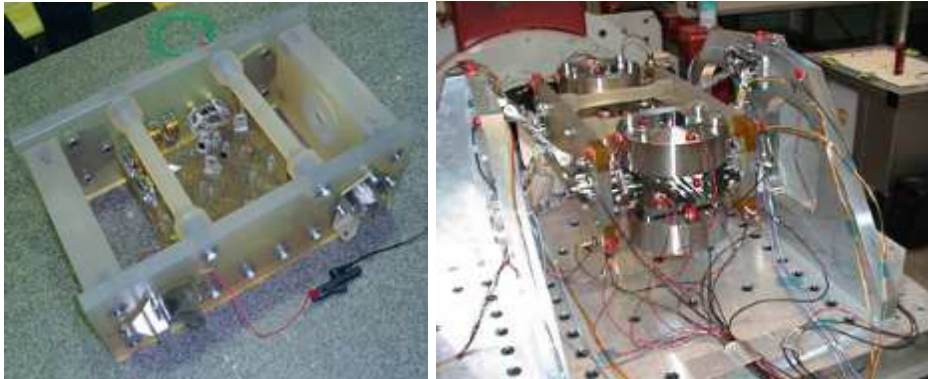


Figure 4. Left: a prototype of the optical bench under development. Right: vibration test of the optical bench with two dummies of the gravity reference sensors to simulate the launch loads.

on the illumination scheme, the generated photoelectrons can be deposited on or taken out of the proof-mass to achieve electrical neutrality.

The absence of a mechanical contact also requires that a blocking mechanism keeps the mass fixed during launch and is able to release it overcoming the residual adhesion. This release must leave the proof-mass with small enough linear momentum to allow the control system described in the following to bring it at rest in the nominal operational working point.

The system formed by one proof-mass, its electrode housing, the vacuum enclosure and the other subsystems is called in the following the gravity reference sensor (GRS).

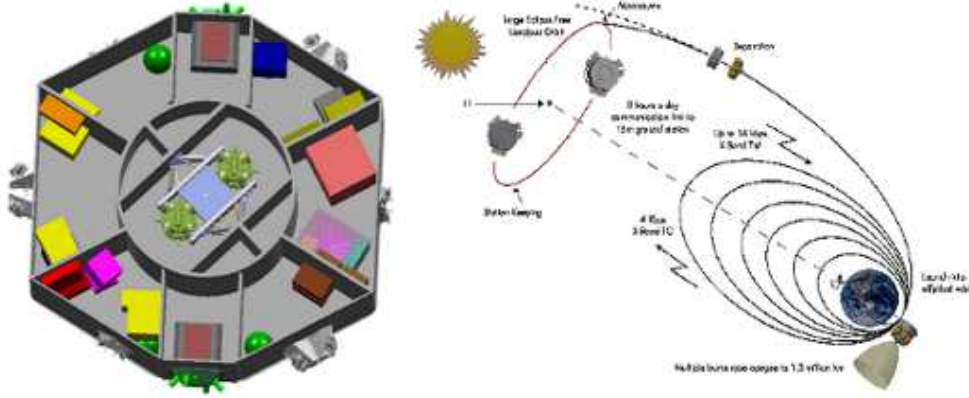


Figure 5. Left: the LTP accommodated within the central section of the LISA Pathfinder spacecraft. Right: the injection of LISA Pathfinder in the final orbit around L1.

The interferometer system provides the following measurements: 1) heterodyne measurement of the relative position of the proof-masses along the sensitive axis. 2) Heterodyne measurement of the position of one of the proof-masses (proof-mass 1) relative to the optical bench. 3) Differential wave-front sensing of the relative orientations of the proof-masses around the y -axis and the z -axis. 4) Differential wave-front sensing of the orientation of proof-mass 1 around the y -axis and z -axis. Sensitivities at mHz frequency are in the range of $10 \text{ pm}/\sqrt{\text{Hz}}$ for displacement and of $10 \text{ nrad}/\sqrt{\text{Hz}}$ in rotation.

As a light source for the heterodyne interferometry, a diode-pumped, monolithic Nd:YAG non-planar ring oscillator is used. To obtain the necessary frequency shift, the beam coming from the laser is split and each partial beam is sent through an acousto-optical modulator (AOM). The light is then delivered to the optical bench by a pair of optical fibres and fibre injectors. Quadrant photo-diodes are used for the detection of the interferometric signal, allowing to measure yaw and pitch of the proof-masses with respect to the sensitive axis. The optical components needed for the interferometer (i.e. mirrors and beam-splitters) are attached to the optical bench through hydroxyl-silicate bonding to ensure mechanical stability.

Data acquisition, conditioning and phase-measurement is performed by the interferometer front-end electronics, based largely on Field Programmable Gate Arrays (FPGA). The final processing and retrieval of the position signals from the phase measurements is performed by the LTP payload computer. A full description of the interferometer for can be found in [19].

The LTP computer also drives and reads-out the set of subsidiary sensor and actuators [20] needed to apply the already mentioned selected perturbations to the proof-masses and to measure the fluctuations of the disturbing fields. Actuators include coils used to generate magnetic field and magnetic field gradients and heaters to vary temperature and temperature differences at selected points of the Gravity Reference Sensor and of the optical bench. Sensors include magnetometers, thermometers, particle detectors and monitors for the voltage stability of the electrical supplies.

The LTP will fly on LISA Pathfinder [21] in 2008. It will be hosted in the

central section of the spacecraft (figure 5, left), where gravitational disturbances are minimized, and will operate in a Lissajous orbit [22] around the Lagrange point 1 of the Sun-Earth system, an environment very similar to that where the LISA spacecrafts will operate (figure 5, right). Further details can be found in [21].

2.2. Experiment performance: similarities and differences with LISA.

Within the LTP, as in LISA, a key element for suppressing the force disturbance is that the proof-masses have no mechanical contact to the spacecraft. In addition, as forces may depend on the position of the proof-masses within the spacecraft, this is kept as fixed as possible.

To fulfill both of these apparently conflicting requirements, [1] the spacecraft actively follows the proof-mass located within it, in a closed loop control scheme usually called the drag-free control. The position of the proof-mass relative to some nominal origin is measured by means of the gravitational reference sensor. A high gain control loop tries to null this error signal by forcing the spacecraft to follow the proof-mass. In order to produce the necessary force on the spacecraft, the control loop drives a set of micro-thrusters.

With this control scheme, if the loop gain is high enough, the difference of force between two masses sitting in two different spacecraft can be calculated [2] to be:

$$\frac{\Delta F}{m} = \frac{\Delta f}{m} - \omega_{p2}^2 \delta x_2 + \omega_{p1}^2 \delta x_1 \quad (13)$$

Here Δf is the difference of position-independent, fluctuating forces directly acting on proof-masses, $\omega_{p1(2)}^2$ is the stiffness per unit mass of parasitic spring coupling of proof-mass 1(2) to the spacecraft and $\delta x_{1(2)}$ is the residual jitter of the same proof-mass relative to the spacecraft.

The LTP experiment uses a similar drag-free control scheme. However here both masses sit in one spacecraft and cannot be simultaneously followed by it. One of them must be forced to follow either the other one or the spacecraft, possibly within a closed loop control scheme. The small required force is applied via the capacitive actuation described above and this control loop is usually called the electrostatic suspension.

Various modes of control are envisaged [23, 24]. In the basic one the spacecraft follows one of the proof-masses, say n.1, along the direction of the interferometer arm. In addition, the main interferometer readout, i.e. the distance between the proof-masses, is used as the error signal to actuate the second proof-mass along the same axis. This way the distance between the proof-masses is kept constant.

The laser interferometer output, at angular frequency ω , is given, in the Fourier space, by:

$$\delta x_{\text{ifo}} = x_{n,\text{ifo}} + \frac{\Delta F}{\omega^2 m} \quad (14)$$

where $x_{n,\text{ifo}}$ is the interferometer displacement noise and the difference of force on the right hand side includes all possible contributions.

$\Delta F/m$ is affected by the control loops. In the approximation of high drag-free gain and small parasitic stiffness, $\Delta F/m$ is given by [14]:

$$\frac{\Delta F}{m} \approx \frac{\omega^2}{\omega^2 - \omega_{\text{es}}^2(\omega)} \left\{ \frac{\Delta f}{m} + (\omega_{p1}^2 - \omega_{p2}^2) \delta x_1 + \omega_{\text{es}}^2(\omega) x_{n,\text{ifo}} \right\} \quad (15)$$

where $\omega_{\text{es}}^2(\omega)$ is the gain (per unit mass) of the electrostatic suspension loop. Δf in the parentheses is again the position-independent difference of forces that would act on the proof-masses *in the absence of any control loop*.

The effective measurement of $\Delta F/m$ is performed by measuring the signal δx_{ifo} , or even better its second time derivative. By using (15) one gets:

$$\omega^2 \delta x_{\text{ifo}} \approx \frac{\omega^2}{\omega^2 - \omega_{\text{es}}^2(\omega)} \left\{ \frac{\Delta f}{m} + (\omega_{p1}^2 - \omega_{p2}^2) \delta x_1 + \omega^2 x_{n,\text{ifo}} \right\} \quad (16)$$

Equation (16) brings a remarkable similarity to (13), thus suggesting that indeed the basic concept of the experiment is sound. However there are a few remarks that need to be done.

In the LTP both proof-masses are spring-coupled to the same spacecraft and both feel then the relative jitter between this one and the drag-free reference proof-mass 1. Some care must then be used to avoid that, by getting $\omega_{p1}^2 \simeq \omega_{p2}^2$ a substantial residual jitter δx_1 becomes unobservable, thus yielding a too small estimate of the noise in (13). This is easily avoided by a detailed sequence of measurements for both ω_{p1}^2 and ω_{p2}^2 that has been described in [14].

Correlation of disturbances on different proof-masses may play a different role in LISA and in the LTP. In LISA proof-masses within the same interferometer arm belong to different spacecraft and are located 5×10^9 m apart. The only correlated disturbances one can think of are connected to the coupling to the Sun: magnetic field fluctuations, fluctuation of the flux of charged particles in solar flares and the fluctuation of solar radiation intensity that may induce correlated thermal fluctuations in distant spacecraft. These correlations will only slightly affect the error budget and will have no profound consequences on the experiment itself.

In the LTP all sources of noise that share the same source for both proof-masses are correlated. Magnetic noise generated on board the spacecraft, thermal fluctuations and gravity noise due to thermo-elastic distortion of spacecraft constitute a few examples. The major concern with correlated noise is that, by affecting the proof-masses the same way, it might subtract from the differential measurement. This subtraction would not happen in LISA and thus would cause an optimistic underestimate of the total noise. This possibility can reasonably be avoided for almost all candidate effects: magnetic disturbances are quadratic function of the field and can then be modulated by purposely applying asymmetric fields and gradient to different proof-masses (that will anyhow have susceptibility and remnant moments only matched not better than 50%). Sensitivity to thermal gradient can be modulated by independently adjusting the static temperature of each proof-mass. Similar strategies of intentional mismatch of the response function of the two proof-masses can be devised for almost all disturbances.

An exception is constituted by the gravitational noise for which the response, due to the equivalence principle, cannot be changed. However realistic assumptions about thermal distortion make the event of a gravity fluctuation affecting both proof-masses with the same force along the \mathbf{x} -axis very unlikely.

In addition LISA Pathfinder also carries the independent NASA provided ST-7 technology package [25], based on the same concept as the LTP that will operate for part of the mission jointly with the LTP. The possibility that these gravitational disturbances cancel exactly and simultaneously on both instruments is even more unlikely if not impossible. Notice that the joint operation between LTP and ST-7 will also allow to detect some of the correlated disturbances discussed above.

The presence of the electrostatic suspension multiplies the forces in (16) by the transfer function $\omega^2 [\omega^2 - \omega_{\text{es}}^2(\omega)]^{-1}$. Though the numerical algorithm behind $\omega_{\text{es}}^2(\omega)$ is entirely known, this gain also includes the conversion from a force command issued by a computer to actual voltages and forces on the proof-masses, thus posing a calibration issue if $|\omega_{\text{es}}^2(\omega)| \gtrsim \omega^2$. If instead $|\omega_{\text{es}}^2(\omega)| \ll \omega^2$, then the $\omega^2 \delta x_{\text{ifo}}$ is a faithful representation of the force signal. This last limit is then accurate and can be used for calibration, but it brings about the disadvantage that $\omega_{\text{es}}^2(\omega)$ must be kept small at all relevant frequencies, thus producing long and slightly unpractical relaxation time constants in the electrostatic suspension loop. As an alternative, within the joint operation with ST-7, a calibration procedure is envisaged where a comparatively large motion of one of the proof-masses of the ST-7 package is used to generate an oscillating gravitational field on the LTP proof-masses. This will allow an independent absolute calibration of forces on board at better than 1%.

Finally (16) shows that the readout noise contributes the feedback force $\omega^2 x_{n,\text{ifo}}$ that is not present in the case of LISA. This is discussed in the next section.

2.3. Experiment performance: sensitivity

As an instrument to measure $\Delta F/m$, the LTP is then limited by the laser interferometer noise. When $|\omega_{\text{es}}^2(\omega)| \ll \omega^2$ the signal is:

$$\omega^2 \delta x_{\text{ifo}} \approx \frac{\Delta f}{m} + (\omega_{p1}^2 - \omega_{p2}^2) \delta x_1 + \omega^2 x_{n,\text{ifo}} \quad (17)$$

Equation (18) shows that, as in LISA, the laser interferometer noise converts into an effective force noise according to

$$S_{\Delta F/m}^{1/2}(\omega) \approx \omega^2 S_{n,\text{ifo}}^{1/2}(\omega) \quad (18)$$

For the LTP the laser interferometer is requested to achieve a sensitivity of:

$$S_{n,\text{laser}} = \left(9\text{pm}/\sqrt{\text{Hz}}\right) \sqrt{1 + \left(\frac{\omega}{2\pi \times 3\text{mHz}}\right)^{-4}} \quad (19)$$

This noise corresponds to an equivalent force noise of:

$$S_{\Delta F/m}^{1/2}(f) \approx \left(3.2 \times 10^{-15} \text{ms}^{-2}/\sqrt{\text{Hz}}\right) \left[1 + \left(\frac{f}{3\text{mHz}}\right)^2\right] \quad (20)$$

At lower frequencies an additional force noise adds up to mask the parasitic forces due to other sources. This force noise is due to the fluctuations of the gain of the electrostatic suspension loop. Indeed the electrostatic suspension must also cope with any static force acting on the proof-masses. If the force stays constant but the gain fluctuates, the feedback force fluctuates consequently, adding a noise source that is expected to limit the sensitivity at the lowest frequencies. This effect only appears in the LTP as in LISA static forces are compensated just by the drag-free loop, and no electrostatic suspension is envisaged. The largest expected source of gain fluctuations is the fluctuation of the dc voltage which is used to stabilize the actuation electronics.

A relative fluctuation of the voltage $\delta V/V$ would then produce a fluctuation of force:

$$\frac{\delta f}{m} \approx \left(\frac{\Delta f}{m}\right)_{\text{static}} \times 2 \frac{\delta V}{V} \quad (21)$$

where the factor 2 comes from the quadratic conversion from voltage to force.

For the LTP it is required that $|\Delta f/m|_{\text{static}} \leq 1.3 \times 10^{-9} \text{ms}^{-2}$. However to keep some margin, balancing of the gravitational field, the largest source of dc forces, is requested at one half of the above figure and current models predict that the remaining sources of dc forces are negligible. In addition the dc-voltage reference is required to be stable to within $S_{\delta V/V}^{1/2} \leq 2 \times 10^{-6} 1/\sqrt{\text{Hz}}$ at 1 mHz. As a goal this stability should degrade not worse than $1/f$ at lower frequencies down to 0.1 mHz. If one can achieve these goals, gain fluctuations may convert to an equivalent force PSD of

$$S_{f_{fb}/m}^{1/2}(f) \approx 1.8 \times 10^{-15} \frac{\text{m.s}^{-2}}{\sqrt{\text{Hz}}} \sqrt{1 + \left(\frac{1\text{mHz}}{f}\right)^2}. \quad (22)$$

Adding up the results in (22) and (20) one gets the sensitivity prediction in figure 6.

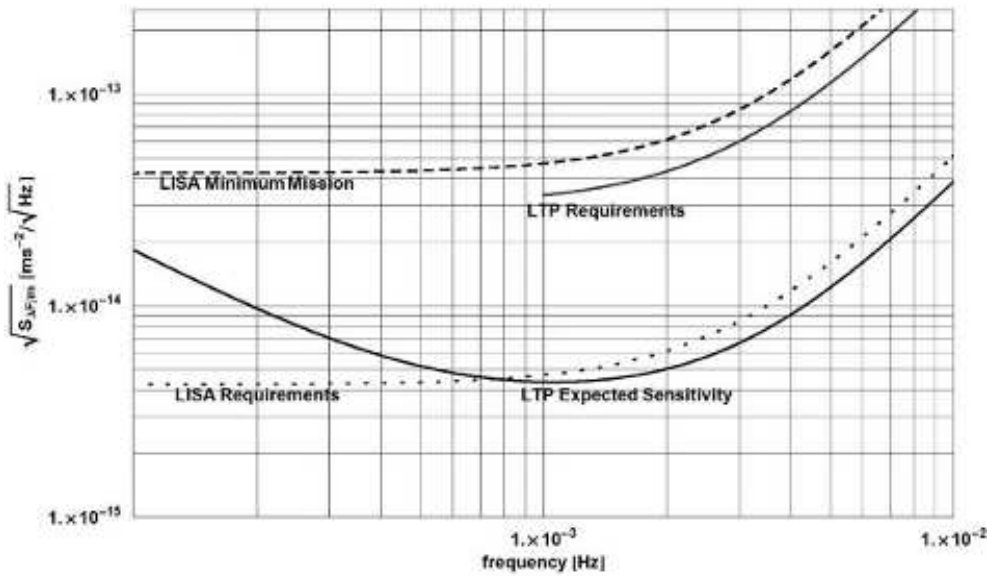


Figure 6. Lower solid curve: projected sensitivity for differential force measurement of the LTP experiment. Upper solid curve: required maximum differential acceleration noise for the LTP. Lower dotted curve: LISA requirements from (8). Upper, dashed curve: LISA Minimum mission requirements.

In figure 6 we also report for comparison, besides the LISA requirements from (8) and the LTP maximum noise requirements, the required sensitivity for mission success for LISA, the so called “minimum mission” requirements. This mission would still detect gravitational waves from merger of black holes with $3 \times 10^5 M_\epsilon$ at $z = 1$ with high S/N ratio. Furthermore it would be able to detect and study the waves from thousands of Galactic compact binaries. Finally it would detect at $\text{SNR} > 10$ one or more of the well identified galactic binaries that are usually called “verification binaries” as everything is known about the expected gravitational wave signal.

3. Concluding remarks

Figure 6 shows that the ultimate uncertainty on the differential acceleration PSD can be potentially constrained by the LISA Pathfinder mission below a factor 5 above LISA requirements at 0.1 mHz, and near LISA requirements at 1 mHz or above.

In addition, within the entire frequency range, the LISA Pathfinder mission will constrain the acceleration noise somewhere in the range between 1 and $10 \text{ fm s}^{-2}/\sqrt{\text{Hz}}$ well below the requirements of LISA minimum mission, thus strongly reducing the risk of a LISA failure.

Notice that the resulting TT frame, a frame where free particles at rest remain at rest, is a very close approximation to the classical concept of inertial frame, and would indeed be inertial, within the measurement bandwidth, wouldn't it be for the presence of the gravitational wave. Thus LISA Pathfinder will demonstrate the possibility of building an inertial frame in a standard spacecraft orbiting the Sun on a scale of a meter in space and of a few hours in time at the above mentioned level of absence of spurious accelerations. To our knowledge this will be at least 2 orders of magnitude better than what will be achieved by the GOCE mission [26] which will in turn be much better than any existing current limit.

References

- [1] Bender P. et al., "LISA Pre-Phase-A report" MPQ 208 (Munich 1996, unpublished).
- [2] Vitale S., et al Nuclear Physics B (Proc. Suppl.) **110**, 209 (2002)
- [3] Misner C. W. , Thorne K. S., and Wheeler J. A. "Gravitation" (Freeman & Co., San Francisco, 1973)
- [4] Stebbins R. T., et al, Class. Quantum Grav. **21** (2004) S653–S660
- [5] Vitale S 2002 LISA Technology Package Architect Final Report ESTEC contract no 15580/01/NL/HB
- [6] Hueller M., et al., Class. Quantum Grav. **19** (2002) 1757–1765
- [7] Carbone L., et al 2003 Phys. Rev. Lett. **91** 151101
- [8] Carbone L. et al., Class. Quantum Grav. **21** (2004) S611–S620
- [9] Carbone L. et al., Class. Quantum Grav. (this issue) to appear (2005); also gr-qc/0412103
- [10] Hueller M. et al., Class. Quantum Grav. (this issue) to appear (2005); also gr-qc/0412093
- [11] Vitale S., and Dolesi R., AIP Conference Proceedings **523**, 231 (2000)
- [12] Cavalleri A., et al., Class. Quantum Grav. **18** (2001) 4133–4144
- [13] Bortoluzzi D., et al., Class. Quantum Grav. **20** (2003) S89–S97
- [14] Bortoluzzi D., et al, Class. Quantum Grav. **21** (2004) S573
- [15] Weber W. J., et al., SPIE Proc. **4856**, 31 (2002)
- [16] Dolesi R., et al., Class. Quantum Grav. **20** (2003) S99–S108
- [17] Mance D., Zweifel, P., "LISA Pathfinder Mission LTP - Inertial Sensor Front-End Electronics" S2-ETH-RS-3001, (ETH- Zurich 2004)
- [18] Sumner T., et al., Class. Quantum Grav. **21** (2004) S597–S602
- [19] Heinzel G., et al., Class. Quantum Grav. **21** (2004) S581–S587
- [20] Lobo A. et al., "Data Diagnostics System science requirements document", S2-IEEC-RS-3002, (IEEC, Barcelona 2004)
- [21] Dunbar N., Tomkins K., Gould K., Lecuyot A., Holt T., Fichter W., "LISA Pathfinder system design synthesis report", S2.ASU.RP.2003 (EADS-ASTRIUM 2004)
- [22] Landgraf M., Heckler M., and Kemble S., Class. Quantum Grav. (this issue) to appear (2005)
- [23] Bortoluzzi D., et al, Class. Quantum Grav. **20** (2003) S227–S238
- [24] Fichter W., et al., Quantum Grav. (this issue) to appear (2005)
- [25] <http://nmp.jpl.nasa.gov/st7/>
- [26] <http://www.esa.int/export/esaLP/goce.html>